# High-pressure single-crystal X-ray diffraction facilities on station 9.8 at the SRS Daresbury Laboratory – hydrogen location in the high-pressure structure of ethanol

**David R. Allan,[a]* Simon Parsons[b] and Simon J. Teat[c]**

*[a]Department of Physics and Astronomy, The University of Edinburgh, Mayfield Road, Edinburgh EH9 3JZ, UK, [b]Department of Chemistry, The University of Edinburgh, Mayfield Road, Edinburgh EH9 3JJ, UK, and [c]CCLRC Daresbury Laboratory, Daresbury, Warrington WA4 4AD, UK. E-mail: dra@ph.ed.ac.uk*

A new high-pressure single-crystal diffraction facility has been constructed on station 9.8 at the Synchrotron Radiation Source, Daresbury Laboratory, for a range of studies on a variety of systems of relevance to physics, chemistry and materials science that would otherwise prove intractable with conventional laboratory-based methods. The station has been equipped with a modified Enraf–Nonius CAD4 four-circle diffractometer for high-pressure studies which can be conveniently, and rapidly, interchanged with the Bruker SMART CCD area-detector system when more routine ambient-pressure diffraction work is to be undertaken. This rapid change-over has been achieved by permanently mounting the CAD4 on its own jacking table, formerly used for the station's white-beam diffraction mode, which allows the alignment of the SMART diffractometer to remain undisturbed when the CAD4 is in use. Early results on the test low-melting-point compound ethanol ($CH_3CH_2OH$) reveal that excellent refined structures can be obtained, including the location and refinement of the H atoms, demonstrating that one of the original, and major, objectives of the station has been accomplished.

**Keywords: high pressure; single-crystal X-ray diffraction; ethanol.**

## 1. Introduction

For ambient-pressure crystallography, single-crystal X-ray diffraction is often sufficient to provide hydrogen positions for small-molecule systems although neutron diffraction (with powders or single crystals) is the method of choice for accurate studies or in cases where detailed thermal displacement parameters are required. In the case of high-pressure single-crystal X-ray diffraction, however, the data quality is often relatively poor, due to the constraints of the diamond-anvil cell both for sample volume and X-ray access, and, where H-atom refinement has been attempted, geometrical constraints are required. High-pressure neutron-diffraction techniques are now well established at both reactor and spallation sources and still provide the best structural information on hydrogenous systems. However, as the sample volumes need to be relatively large to provide sufficiently intense diffracted intensities, many high-pressure phases are inaccessible due to the limited pressure range available (approximately 30 GPa with the Paris–Edinburgh cell, though this is further limited to about 1 GPa for liquid samples that have not yet crystallized). Additionally, powder diffraction is the most commonly used technique for high-pressure neutron studies and this can lead to difficulties when a crystalline phase is formed directly from the liquid on compression. As the resulting crystallites can be relatively large and often share a common growth direction, such samples usually exhibit severe preferred orientation and texture effects leading to poor powder averaging.

High-pressure powder-diffraction studies, with the limited sample volumes available from diamond-anvil cells, are well suited to the high X-ray fluxes available at synchrotron radiation sources and recent work has provided unprecedented accuracy and detail for systems containing relatively strong scatterers, such as elemental metals and semiconductors. In contrast, high-pressure single-crystal diffraction has remained almost exclusively based at in-house laboratories with sealed-tube sources. Here we report a preliminary high-pressure single-crystal study conducted on station 9.8 at the Synchrotron Radiation Source (SRS), Daresbury Laboratory, and developments on the station to allow such work to be conducted routinely. We have selected ethanol for this initial study as we have already determined its high-pressure structure (Allan & Clark, 1999); it crystallizes readily on compression and good quality single crystals can be grown relatively easily by cycling the temperature close to the melting point.

## 2. High-pressure configuration of the station

It has been a long-standing aim that station 9.8 at SRS, Daresbury Laboratory, should provide facilities for high-pressure single-crystal diffraction as the high X-ray flux, particularly at short wavelengths ($\lambda < \sim 0.7$ Å), is ideal for the study of weakly scattering systems contained within diamond-anvil cells. The station set-up has been described previously in great detail elsewhere (Cernik *et al.*, 1997) and only the recent developments for high-pressure studies will be outlined here. During the commissioning of station 9.8, two detector systems were provided: a Bruker AXS SMART CCD area detector, complete with a three-circle fixed-$\chi$ goniometer and associated control electronics and software, for general small-molecule crystal-structure determinations; and an Enraf–Nonius CAD4 kappa-geometry diffractometer with a scintillation counter for non-routine studies, specifically high-pressure work. In the initial stages the station was capable of carrying out energy-dispersive powder diffraction and Laue crystallography, formerly undertaken on station 9.7, and, so that the 9.8 hutch could offer the dual capability of monochromatic and white-beam diffraction modes, the station was equipped with two jacking tables: the first to house either one of the diffractometers at the focal point of the mirror and the focusing Si(111) monochromator; the second for an energy-dispersive set-up at a position approximately 1 m closer to the source. With the recent commissioning of the white-beam

  

station 16.4 at SRS, the energy-dispersive mode of the 9.8 hutch was made redundant, allowing the second jacking table to be put to another use. Although, as already stated, this table is not positioned at the focus of the X-ray beam, it was considered to be an excellent compromise to permanently mount the CAD4 diffractometer here as the loss of X-ray flux would not be prohibitive and would allow a rapid changeover (see Fig. 1). As the second table is positioned between the SMART and the source, the CAD4 must be translated out of the beam when not in use. The lateral translating jacks on the table do not provide sufficient movement and, as a consequence, the CAD4 diffractometer is mounted on a pair of rails so that it can be rolled to a parking position between experiments. In order that this translation can be made reproducible, a set of stops are provided to allow the diffractometer to be locked firmly in both the 'parked' and 'beam' positions. There is sufficient clearance in the parked position to enable a long evacuated beam-pipe to be mounted for the SMART diffractometer. In the beam position this beam-pipe is replaced with a shorter version. During this change-over, the alignment of the SMART is completely unaffected and it can therefore be used almost immediately when the CAD4 is parked. Provided that the station X-ray optics have not been adjusted while the SMART has been in use, the re-positioning of the CAD4 onto the beam will only require a minor realignment with the jacking table.

### 2.1. *Alignment*

If the X-ray optics have had substantial adjustments between change-overs, an initial crude alignment of the CAD4 may be required. This is usually undertaken by fixing the position of the beam with 'green' paper and then positioning the table in vertical and lateral directions until the beam passes through the upstream end of the shutter/collimator housing. With this preliminary alignment completed, the diffractometer is scanned across the beam, in both the vertical and horizontal, so that the intensity passing through the collimator, and recorded with an ion-chamber, is maximized. The fore and aft vertical and lateral jacks are also adjusted in opposition, while monitoring the X-ray flux, to allow the table to be tilted and rotated so that the collimator can be made parallel to the beam. This procedure is repeated with progressively smaller diameter collimators so that the alignment is sufficiently good for final fine alignment with the test crystal. A 200 μm ruby sphere is used for this purpose in conjunction with the CAD4 *ALIGN* procedure (King & Finger, 1981). The *ALIGN* procedure provides alignment errors for the tube and monochromator, when the diffractometer is mounted on a conventional laboratory source, by measuring the setting angles of a standard reflection (required to have $80^\circ < \chi < 110^\circ$ for a kappa-geometry machine) at Hamilton's eight equivalent diffractometer positions (King & Finger, 1981). With the tube and monochromator adjusted appropriately, the *ALIGN* procedure is repeated until the alignment errors are deemed suitably small. For station 9.8, the vertical tube error (TubeVe) from *ALIGN* gives a measure of the rotation error of the jacking table, and the fore and aft horizontal-translation jacks are adjusted in opposite senses so that its value is minimized. Similarly, the horizontal tube error (TubeHo) gives a measure of the tilt error of the diffractometer, and the fore and aft vertical-translation jacks must be adjusted in opposition to eliminate this error. Final errors of no more than 0.05 mm for TubeVe and TubeHo are usually found to be acceptable, and for additional accuracy the collimator with the smallest internal diameter (1 mm) is used. If large initial errors for either TubeVe or TubeHo are found, it is necessary to adjust the global vertical and horizontal positioning of the diffractometer to ensure that the collimator remains centred in the X-ray beam.

With the diffractometer accurately aligned, the setting angles of up to 25 ruby reflections are determined accurately with the *SET4* routine. This measures the setting angles of selected reflections at four equivalent positions on the diffractometer to eliminate any residual crystal centring errors or minor aberrations in the diffractometer alignment. Finally, the list of setting angles produced in this manner is used to determine the X-ray wavelength accurately.

### 2.2. *Sample reflection search procedure*

The strong and textured background produced by the illuminated components of a diamond-anvil cell makes the use of a random sample reflection search impractical. The diffract-

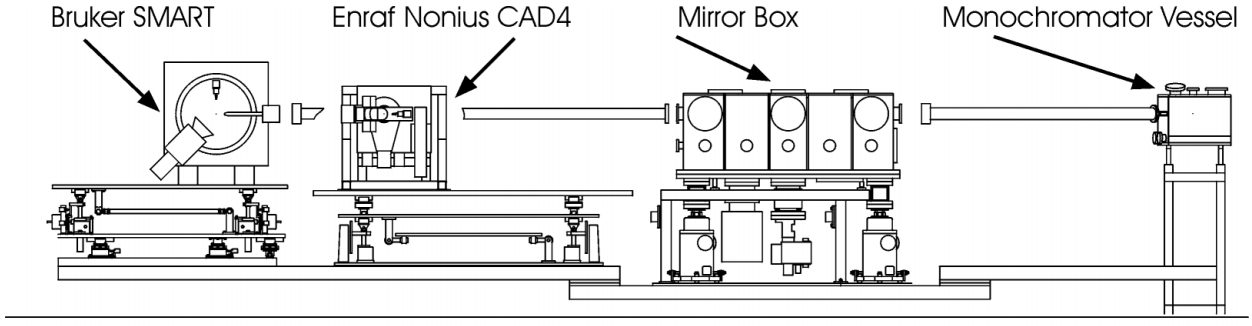


**Figure 1**
Layout of the experimental hutch for station 9.8, showing the large pivot arm about the monochromator and carrying the mirror and diffractometer systems.

ometer may often centre on diamond reflections or reflections from large beryllium grains in the diamond backing discs. For laboratory-based high-pressure single-crystal X-ray diffraction, a polaroid rotation photograph is often taken prior to a more targeted search. The spots on the developed photograph from sample reflections are strikingly different in appearance from those due to diamond reflections and it is therefore relatively straightforward to discriminate between them. By measuring quartets of symmetry-related spots on the photograph, and with a knowledge of the camera-to-sample distance, a list of $2\theta$ and $\chi$ values can be constructed for the strongest sample reflections. By driving the diffractometer to $2\theta$, $\omega$ (= $\theta$) and $\chi$, a search on only the $\varphi$-axis is then required, which invariably locates the required sample reflection. We have adopted a similar search strategy for the CAD4 diffractometer on station 9.8. A detachable bracket has been constructed to hold an A4-sized image plate at a distance of 220 mm from the sample position. An exposure time of approximately 10 min is sufficient to harvest a sufficient number of sample reflections for an initial orientation matrix determination, even when the unit cell is initially unknown.

### 2.3. *Data-collection strategy and beam-decay correction*

A crucially important consideration when planning a single-crystal data collection on a synchrotron is the provision of a means of measuring the decay of the X-ray beam (due to the unavoidable loss of electrons in the storage ring) which must be corrected for before the data can be analyzed successfully. Ambient-pressure data collections with the SMART diffractometer can be corrected for this effect by monitoring the incident beam with an upstream ion chamber as the detector frames are collected or, more usually, the correction is applied after data collection with the *SADABS* program (Sheldrick, 1997). The success of this latter strategy is due, in part, to the large number of reflections that can be collected simultaneously with the CCD area detector and the resulting redundancy in the raw intensity data set. For the CAD4, the reflections must be measured individually and in a predetermined sequence to reduce the diffractometer sluing time. Consequently, each reflection will be measured with a different incident intensity depending on its position (or time from the start of the data collection) in the sequence. It is possible, however, to determine the rate of beam decay by measuring a set of standard reflections at pre-determined intervals during data collection. These standard reflections are written as profiles to the raw intensity data file along with the time, in seconds, that the reflection was measured from the start of the data collection. In the same way, the profiles of the 'normal' reflections are recorded in sequence and the time that each was measured is also written to the file. The data file, therefore, is composed of a sequence of records containing, among other details, a flag for either intensity control or normal reflection ($I$ or $N$, respectively), the time in seconds from the start of the data collection and the profile, stored as a sequence of 96 bins. When the data are reduced, usually with the Lehmen–Larson routine (Lehmann & Larsen, 1974), the intensity of each integrated profile, its time and its status ($I$ or $N$) can be recorded. By fitting a polynomial function to the intensity of each of the standard $I$ reflections with time (usually a set of three is measured), the beam decay can be estimated as a function of time for the duration of the data collection. The normal $N$ reflections can then be corrected for beam decay using this polynomial and the time-stamp on each of the reflection's raw data file record. Intensity controls are automatically measured at the start and end of each data collection and experience has shown that re-measuring the intensity controls in half-hour intervals, for a typical 20 hour data collection, provides a sufficient number of points to determine the polynomial accurately.

As the dynamic range of the CAD4 intensity measurements is severely limited by the $10^4$ count limit of the profile bins in the raw data file, care has to be taken to ensure that format overflows are not encountered during data collection, an extremely important consideration for the $I$ reflections. This problem is exacerbated by the low divergence of the synchrotron beam which reduces the widths of the reflections and can concentrate a substantial proportion of a reflection's intensity into only a few bins. Although the scan widths can be reduced to minimize these effects, the inaccuracies of the orientation matrix, especially when the sample is held in a diamond-anvil cell, require that the scan widths are not reduced so much that the profile is no longer correctly centred. By performing a series of short test data collections, appropriate scan widths and scan durations can be determined for the sample under investigation.

With the sample correctly centred on the CAD4 goniometer, an accurate orientation matrix measured, and the durations and widths of the intensity-scans determined, a full data collection can be initiated. For high-pressure studies, the reflections are measured at the position of least attenuation by the diamond-anvil cell which requires the rotation axis of the cell (*i.e.* the normal to the diamond culets) to be set in the diffraction plane of the diffractometer. Conventionally this requires each reflection to be measured at the non-bisecting fixed-$\varphi$ position. If the cell is mounted so that its axis is set parallel to the incident beam direction, when all the goniometer circles are at zero, then the $\varphi$-axis is set equal to 0° during each intensity scan. The CAD4 control software incorporates a routine to determine (*a*) which reflections are accessible when the diamond-anvil cell is used, and (*b*) the angle around the diffraction vector $\psi$ that the reflection must be measured so that the $\varphi$-axis is set to 0° (or in some instances 180°). The textured background generated by illuminated cell components can also produce spurious peaks in conventional $\omega/2\theta$ intensity scans, making accurate profile integration extremely difficult if not impossible. To minimize this effect it is normal practice to measure the reflection intensities with $\omega$-scans so that the detector is not scanned over a beryllium powder-diffraction line which would then produce a peak in the profile. If the detector remains stationary on a powder line, as would occur during an $\omega$-scan, then only an enhanced, but flat, background would be measured. The standard CAD4 control software already provides this important option.

## 3. Test results – hydrogen location in the high-pressure structure of ethanol

We have conducted high-pressure single-crystal X-ray diffraction studies of the monoalcohols methanol ($CH_3OH$) and ethanol ($CH_3CH_2OH$) to initially determine which features in their high-pressure crystal structures explain why methanol often vitrifies on compression while ethanol readily crystallizes. For ethanol, we find that the O—H···O bond angles in the high-pressure structure are equal by symmetry and are close to the ideal value of 180° (Allan & Clark, 1999) while, by contrast, those of the high-pressure phase of methanol (Allan *et al.*, 1998) range from 150.9° to 178.2°. It was concluded that the hydrogen-bonded chains of methanol molecules were highly strained relative to the high-pressure structure of ethanol, and this apparently leads to the likelihood of glass formation from the liquid on compression.

In this initial high-pressure single-crystal X-ray diffraction work, which was conducted on a standard laboratory sealed-tube source, the H-atom positions were not determined directly but, rather, they were calculated using fully quantum mechanical *ab initio* pseudo potential methods. However, to provide a suitably rigorous test of these and similar calculations, it is important that the location of the H atoms should be determined directly. As the pressures at which both methanol and ethanol crystallize from the liquid at room temperature are somewhat beyond the scope of contemporary neutron-diffraction high-pressure cells, diamond-anvil cells are required in conjunction with synchrotron-based single-crystal X-ray diffraction techniques. Given that methanol is difficult to crystallize at high pressure, we have selected ethanol for this initial study as it can be crystallized readily on compression and good quality single crystals can be grown relatively easily. Additionally, the high-pressure phase of ethanol has a less complex structure as it has only one molecule in the asymmetric unit rather than the three non-symmetry-related molecules in the high-pressure structure of methanol.

### 3.1. *Experiment and data analysis*

Preliminary and final alignment of the station was undertaken using the methods described above having initially scanned the monochromator to the Zr absorption edge. This was achieved by placing a Zr foil in the beam and by monitoring the transmitted signal with an ion chamber as the monochromator crystal angle was varied. The monchromator bend was also adjusted so that the width of the edge, as determined by its range in monochromator angle, was minimized thus producing the optimum wavelength discrimination ($\Delta\lambda/\lambda$). The monochromator angle was finally set at the point of inflexion on the Zr absorption edge. Once the diffractometer itself was fully aligned, the wavelength was determined to be $\lambda = 0.69031\ (1)$ Å with the ruby test crystal.

The sample was prepared by pressurizing liquid ethanol in a Merrill–Bassett diamond-anvil cell (Merrill & Bassett, 1974) which had been equipped with 600 μm culet diamonds and a tungsten gasket. After the nucleation of many crystallites, the temperature was cycled close to the melting curve, in order to reduce the number of crystallites, in a manner similar to the methods used by Vos *et al.* (1992, 1993). Finally, a single crystal was obtained at 2.75 (5) GPa that entirely filled the 200 μm gasket hole.

The cell was transferred to the CAD4 on station 9.8 and the setting angles of 25 strong reflections were determined accurately using the *SET4* routine (see above). A least-squares fit gave the monoclinic unit-cell parameters to be $a = 7.6311\ (5)$ Å, $b = 4.7778\ (4)$ Å, $c = 7.3148\ (5)$ Å, $\beta = 114.87\ (8)°$ and $V = 242.0\ (3)$ Å$^3$, which are in good agreement with our laboratory-based determination (Allan & Clark, 1999). The unit-cell volume from this study, however, is marginally larger, by about 1.2%, than the previously determined 3.0 GPa experimental value (Allan & Clark, 1999) and may reflect the 0.25 GPa pressure difference between the two studies and residual uncertainties in the wavelength determination.

Intensity data were collected with the $\omega$-scan method at the position of least attenuation of the pressure cell, according to the fixed-$\varphi$ technique (Finger & King, 1978). All accessible reflections were measured in the shell $+h, \pm k, \pm l$ for $0\ \text{Å}^{-1} < \sin\theta/\lambda < 0.71\ \text{Å}^{-1}$, including three intensity-control reflections which were measured in half-hour intervals throughout the duration of the data collection, which was completed during a single multi-bunch fill of the synchrotron. The intensities were subsequently corrected for beam decay using a three-term polynomial fit to the intensity control reflections.

Single-crystal intensity data collected from a sample contained within a diamond-anvil cell are confined to an annular volume of reciprocal space (Merrill & Bassett, 1974) and are consequently quasi two-dimensional in nature. This results in a data set with relatively poor resolution along a direction parallel to the rotation axis of the diamond-anvil cell. Although the loss of resolution does not usually prevent structure solution, it often prevents the refinement of full anisotropic displacement parameters and makes interpretation of electron density maps particularly difficult. As the crystal used for the original structure solution (Allan & Clark, 1999) had an orientation within the diamond-anvil cell that is orthogonal to the crystal used in this study, we have elected to merge both data sets to produce fully three-dimensional data. The resulting data set has 749 unique reflections.

The data were corrected for absorption and used for an initial refinement using the carbon and oxygen structural parameters of Allan & Clark (1999) as starting values, and the atoms were refined with full anisotropic displacement parameters (*CRYSTALS*; Watkin *et al.*, 1999). H atoms were located in a difference synthesis based on phases derived from the C and O positions. While the methyl and methylene H-atom positions were clearly visible, there were two peaks in close proximity to the O atom (see Fig. 2). This was interpreted as being indicative of disorder in the H-atom position. In subsequent refinement cycles, similarity restraints were placed on chemically equivalent bond distances and angles involving C and H atoms; the two part weight O—H bonds were restrained to have bond lengths of 0.8 Å but with fairly generous tolerances. Relative occupancies of the part weight H atoms were refined; all H atoms were constrained to have

**Table 1**
Details of the final refinement statistics.

| | |
|---|---|
| Space group | $P2_1/c$ |
| $Z$ | 4 |
| Number of unique reflections | 749 |
| With $F^2 > 2\sigma(F^2)$ | 181 |
| Number of parameters | 52 |
| $R_{int}$ | 0.11 |
| $R$ | 0.0652 |
| $wR$ | 0.0732 |
| $S$ | 1.0156 |

equal isotropic displacement parameters. Final refinement statistics are listed in Table 1.

### 3.2. *Results and discussion*

It is clear from Table 2 that the results of the refinement of the C and O atoms are in good agreement with the values obtained from the theoretical *ab initio* calculations, as are the cell dimensions [which the calculations gave to be $a$ = 7.606 Å, $b$ = 4.754 Å, $c$ = 7.278 Å, $\beta$ = 116.92 (8)° and $V$ = 234.8 (3) Å$^3$ (Allan & Clark, 1999)], subject to the 0.25 GPa pressure difference (see above). The full structure of ethanol at 2.75 GPa, including the experimentally determined positions of the H atoms, is shown in Fig. 3. It can be seen that the molecules form linear hydrogen-bonded chains parallel to the *b*-axis, and within each chain the molecules are coplanar and are aligned parallel to one another in an alternating 1–1–1 sequence (Fig. 4). The molecules are linked in each chain so that their methyl groups are aligned in the same direction along the *b*-axis so that an 'interlocking' arrangement is formed, and they are disordered so that both *trans* and *gauche* conformers are present. The refined occupancies for the *trans* H11 and *gauche* H12 are 0.7 (1) and 0.3 (1), respectively. The neutron powder-diffraction results of Jönsson (1976) revealed a similar behaviour for the monoclinic *Pc* low-temperature phase. In this structure there are two ordered crystallographically independent *trans* and *gauche* molecules in the unit cell. The torsion angles at the C—O bond are $\tau$[C—C—O—H] = 179 (2)° and $\tau$[C—C—O—H] = −63° for the *trans* and *gauche* conformers, respectively, and their values deviate by less than 4$\sigma$ from those required for an ideal staggered

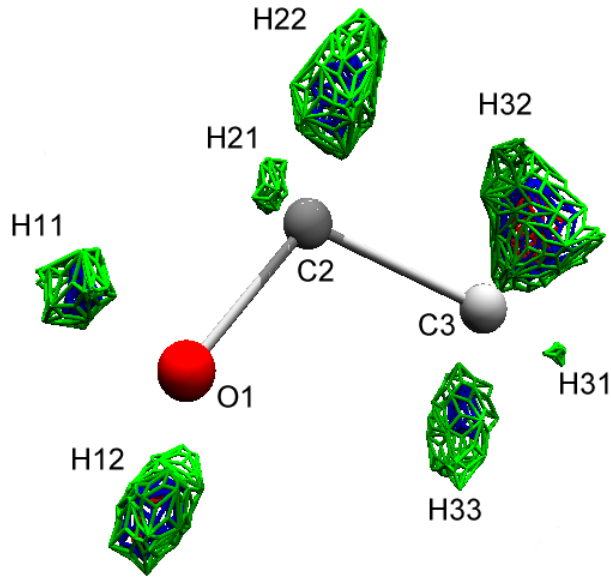


**Figure 2**
A three-dimensional representation of the electron density map surrounding the C and O atoms. Figure produced using *Marching Cubes* (Husak, 1999).

conformation. The corresponding torsion angles for the high-pressure phase are $\tau$[C3—C2—O1—H11] = 177 (4)° and $\tau$[C3—C2—O1—H12] = −44 (9)° for the *trans* and *gauche* conformers, respectively. The torsion angle for the *trans* conformer is in excellent agreement with the low-temperature structure and is close to that required for ideal staggering. However, the torsion angle for the *gauche* conformer is determined less precisely and has a correspondingly poorer agreement, though this is still within about 2$\sigma$.

In Table 3 we give a selection of bond lengths and angles for the high-pressure structure of ethanol as found by both experimental and theoretical methods. To illustrate the distortion of the molecules within the crystal, and to further check our experimental observations, we include the bond lengths obtained from *ab initio* calculations of the gas-phase ethanol molecule. It can be seen that the bonds associated with

**Table 2**
Fractional coordinates of the high-pressure monoclinic $P2_1/c$ ethanol structure obtained from the single-crystal X-ray diffraction results (first set of coordinates) and from the *ab initio* calculations [second set, from Allan & Clark (1999)].

The standard deviations from the single-crystal refinements are shown in parenthesis.

| | Experimental | | | Theoretical | | |
|---|---|---|---|---|---|---|
| | $x$ | $y$ | $z$ | $x$ | $y$ | $z$ |
| O1 | 0.9344(5) | 0.2950 (10) | 0.1622 (6) | 0.9429 | 0.2763 | 0.1750 |
| H11 | 0.952 (5) | 0.462 (9) | 0.188 (8) | 0.9872 | 0.4627 | 0.2312 |
| H12 | 0.933 (11) | 0.18 (3) | 0.239 (15) | | | |
| C2 | 0.7515 (8) | 0.2786 (13) | −0.0015 (8) | 0.7691 | 0.3003 | 0.0076 |
| H21 | 0.660 (2) | 0.363 (3) | 0.034 (3) | 0.6631 | 0.4124 | 0.0456 |
| H22 | 0.755 (2) | 0.372 (3) | −0.113 (3) | 0.7877 | 0.4222 | −0.1103 |
| C3 | 0.6995 (7) | −0.0200 (12) | −0.0541 (8) | 0.6950 | 0.0142 | −0.0704 |
| H31 | 0.695 (6) | −0.112 (4) | 0.058 (3) | 0.6629 | −0.1058 | 0.0385 |
| H32 | 0.793 (4) | −0.103 (4) | −0.088 (5) | 0.7995 | −0.1006 | −0.1067 |
| H33 | 0.579 (3) | −0.029 (3) | −0.163 (4) | 0.5575 | 0.0344 | −0.2112 |

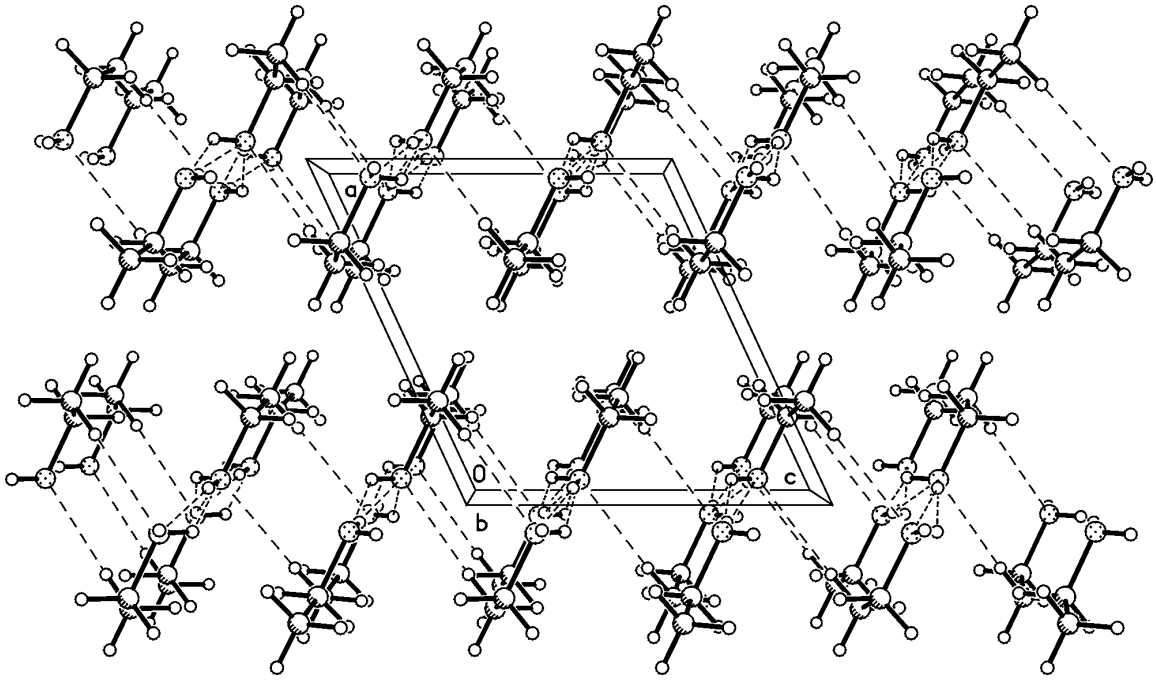


**Figure 3**
The structure of crystalline ethanol at 2.75 GPa.

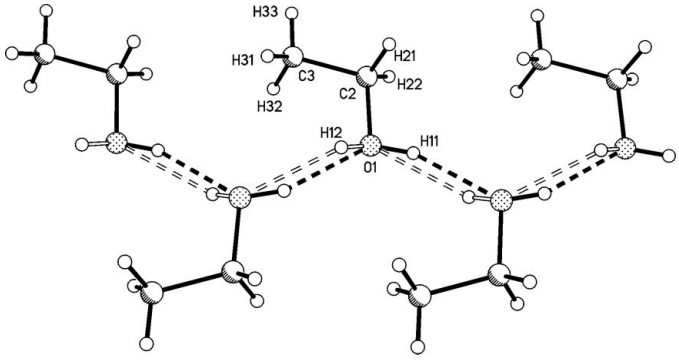


**Figure 4**
The nature of the hydrogen-bonded chains in the high-pressure $P2_1/c$ structure of ethanol at 2.75 GPa. Both the *trans* (bold dashed lines) and *gauche* (double dashed lines) forms are shown.

the H atoms obtained from the experimental data are consistently shorter than the theoretical values: the average C—H methyl distances are 0.937 (18) Å compared with 1.09 Å; the methylene group C—H average distances are 0.936 (18) Å compared with 1.10 Å; and the *trans* O—H distance is 0.82 (4) Å compared with the theoretical value of 0.97 Å for the solid. This apparent shortening of the bonds is about 0.15 Å (approximately 14%) for the C—H distances. The O—H distance is also significantly shorter, again by about 0.15 Å, than predicted by the calculations. However, our experimental values compare more favourably with those obtained for the monoclinic *Pc* low-temperature phase obtained with neutron powder-diffraction by Jönsson (1976). The corresponding O—H distances were found to be 0.79 (4) Å and 0.85 (3) Å at 87 K for the *trans* and *gauche* conformers, respectively. Our experimental values for the *trans* O1—H11 and *gauche* O1—H12 are in excellent agreement with these bond lengths. The average C—H distances for the neutron diffraction study are 0.99 (3) Å and 0.98 (3) Å for the methyl and methylene groups, respectively, which agree closely with our results (*i.e.* to within 5% for both the methyl and the methylene groups). The discrepancy of the *trans* O—H bond length from our present study with the theoretical values is also reflected in the O—H···O and H—O—C bond angles which also differ significantly from the theoretical calculations for the solid. However, the *trans* H—O—C bond angle is in extremely good accord with the gas-phase calculations and both the *trans* and *gauche* bonds are in excellent agreement with the bond angles obtained from the neutron powder-diffraction study, which are 107° and 102° for the *trans* and *gauche* conformers, respectively.

The reasonable agreement between the intramolecular bond lengths and bond angles for the neutron-diffraction results, the gas-phase *ab initio* calculations and the present single-crystal X-ray diffraction study strongly suggests that there may be some deficiency in the *ab initio* calculations of the full crystalline structure. Certainly, the O—H···O hydrogen bond is the most difficult to model accurately as its formation depends on a range of competing factors, with each having a profound effect on the bonding geometry. As the *trans* H—O—C bond angle is in close accord with the gas-phase calculation and the neutron diffraction results, the present work suggests, therefore, that the hydrogen has a much closer affinity to the donor oxygen than was expected by the calculations (*i.e.* the O—H bond was found to be stronger

**Table 3**
Selected bond lengths (Å) and bond angles (°) of the high-pressure structure of ethanol from the experimental studies and the *ab initio* calculations [from Allan & Clark (1999)].

For comparison, corresponding bond lengths and bond angles of *ab initio* calculations for an isolated molecule are also given to show the distortion of the molecule in the crystal as compared with the ideal gas-phase structure [from Allan & Clark (1999)].

| Bond | Experimental | *Ab initio* | Isolated molecule |
|---|---|---|---|
| O1···H11 | 2.06 (4) | 1.626 | |
| O1—H11 | 0.82 (4) | 0.970 | 0.958 |
| O1···H12 | 1.92 (5) | | |
| O1—H12 | 0.80 (5) | | |
| C2—O1 | 1.408 (7) | 1.336 | 1.403 |
| C2—C3 | 1.487 (8) | 1.484 | 1.498 |
| C2—H21 | 0.936 (18) | 1.101 | 1.101 |
| C2—H22 | 0.967 (18) | 1.097 | 1.101 |
| C3—H31 | 0.944 (18) | 1.091 | 1.092 |
| C3—H32 | 0.937 (18) | 1.091 | 1.092 |
| C3—H33 | 0.931 (18) | 1.087 | 1.092 |
| Angle | | | |
| O1—H11···O1 | 135 (1) | 178.8 | |
| H11—O1—C1 | 104.9 (9) | 132.5 | 110.0 |
| O1—H12···O1 | 159 (1) | | |
| H12—O1—C1 | 105.0 (9) | | |
| O1—C1—C2 | 109.1 (5) | 108.5 | 108.3 |

than expected relative to the O···H contact). The theoretical calculations were also based on a structure with only ordered *trans* molecules and not the disordered structure found here, which would be difficult to model with the fully quantum mechanical *ab initio* calculations. Nevertheless, we anticipate that the disorder will have only a limited effect on the nature of the hydrogen bonding in the *trans* conformer and our study has, therefore, provided a stringent test for the computational methods used and our detailed understanding of the nature of the bonding, a central aim of these high-pressure studies.

## 4. Conclusions

We have demonstrated, with the example ethanol study, how the new developments on the station provide an excellent facility for high-pressure studies. Although it is difficult to make a direct comparison between this study and the previous high-pressure study conducted on a standard laboratory sealed-tube source (Allan & Clark, 1999), the standard uncertainties in the refined coordinates and the derived geometrical parameters (bond lengths and bond angles) for the C and O atoms are nevertheless smaller than those of the original result by at least a factor of two. It is expected that further gains in precision (and accuracy) can be achieved with further hardware and software developments on the station. Certainly, the $10^4$ count limit of the profile bins in the raw data file is a severe limitation on the effective dynamic range of the detector and a much larger count range is essential for further improvements in precision.

With the current set-up, the CAD4 diffractometer requires an approximately 6 h overhead for alignment at the start of the experiment. Once fully aligned, however, data collections can be undertaken as a matter of routine and it is possible to collect complete data sets for relatively simple structures (such as that of the $P2_1/c$ phase of ethanol) in a single fill of the SRS (~20 h). For longer data collections, separate data sets spanning two or more fills may be required and each set will need to be scaled appropriately. More recently we have developed high-pressure single-crystal techniques for a SMART diffractometer mounted on a sealed-tube source (Allan *et al.*, 2000). This work revealed that much higher quality data sets can be collected in only a fraction of the time than would be required on a conventional point-detector diffractometer. Just as significantly though, the time required to collect a relatively complex structure (*i.e.* a structure with a large unit cell) is just the same as that required for a simple structure and an identical data-collection strategy would be required. We have now made preliminary high-pressure studies with the SMART diffractometer on station 9.8 which has produced extremely favourable results. The work has shown, however, that for relatively simple systems, such as ethanol, the CAD4 diffractometer is actually more efficient while also providing a greater coverage in $\sin\theta/\lambda$.

We wish to express our thanks to Dr D. J. Taylor of the SRS Daresbury Laboratory for his assistance in the initial alignment of the station during the high-pressure ethanol study. We thank the CCP14 secretary Mr L. M. D. Cranswick and also Mr I. Burrows, both at Daresbury Laboratory, for their help in preparing two of the figures. In addition, we are grateful to Dr S. A. Belmonte for coding the beam-decay correction algorithm into our reflection profile integration code. This work was supported by funding from the EPSRC and CCLRC.

## References

Allan, D. R. & Clark, S. J. (1999). *Phys. Rev. B*, **60**, 6328–6334.
Allan, D. R., Clark, S. J., Brugmans, M. J. P, Ackland, G. J. & Vos, W. L. (1998). *Phys. Rev. B*, **58**, R11809–R11812.
Allan, D. R., Clark, S. J., Parsons, S. & Ruf, M. (2000). *J. Phys. Condens. Matter*, **12**, L613–L618.
Cernik, R. J., Clegg, W., Catlow, C. R. A., Bushnell-Wye, G., Flaherty, J. V., Greaves, N., Burrows, I., Taylor, D. J. & Hamichi, M. (1997). *J. Synchrotron Rad.* **4**, 279–286.
Finger, L. W. & King, H. E. (1978). *Amer. Mineral.* **63**, 337–342.
Husak, M. (1999). *Marching Cubes.* Prague Institute of Chemical Technology, Prague, Czechoslovakia.
Jönsson, P. G. (1976). *Acta Cryst.* B**32**, 232–235.
King, H. E. & Finger, L. W. (1981). *High-Pressure Crystallography with a CAD4.* Instruction Manual. Enraf–Nonius, Delft, The Netherlands.
Lehmann, M. S. & Larsen, F. K. (1974). *Acta Cryst.* A**30**, 580–584.
Merrill, L. & Bassett, W. A. (1974). *Rev. Sci. Instrum.* **45**, 290–294.
Sheldrick, G. M. (1997). *SADABS. Program for Scaling and Correction of Area Detector Data*, University of Göttingen, Germany [Based on the method of Blessing, R. H. (1995). *Acta Cryst.* A**51**, 33–38.]

Vos, W. L., Finger, L. W. & Hemley, R. J. (1992). *Nature (London)*, **358**, 46–48.
Vos, W. L., Finger, L. W. & Hemley, R. J. (1993). *Phys. Rev. Lett.* **71**, 3150–3153.
Watkin, D. J., Prout, C. K., Carruthers, J. R., Etteridge, P. W. & Cooper, R. I. (1999). *CRYSTALS.* Issue 11. Chemical Crystallography Laboratory, University of Oxford, Oxford, UK.


Received 12 October 2000 • Accepted 24 November 2000